

Magnetic phase transitions and magnetoelastic coupling in $S = \frac{1}{2}$ Heisenberg antiferromagnets

Amal al-Wahish,¹ K. R. O'Neal,¹ C. Lee,^{2,3} S. Fan,⁴ K. Hughey,¹ M. O. Yokosuk,¹ A. J. Clune,¹ Z. Li,⁵ J. A. Schlueter,^{6,7} J. L. Manson,⁸ M.-H. Whangbo,⁹ and J. L. Musfeldt^{1,4}

¹Department of Chemistry, University of Tennessee, Knoxville, Tennessee 37996, USA

²Department of Chemistry, Pohang University of Science and Technology, Pohang 790-784, Korea

³Division of Advanced Nuclear Engineering, Pohang University of Science and Technology, Pohang 790-784, Korea

⁴Department of Physics and Astronomy, University of Tennessee, Knoxville, Tennessee 37996, USA

⁵National High Magnetic Field Laboratory, Tallahassee, Florida 32310, USA

⁶Materials Science Division, Argonne National Laboratory, Argonne, Illinois 60439, USA

⁷Division of Materials Research, National Science Foundation, Arlington, Virginia 22230, USA

⁸Department of Chemistry and Biochemistry, Eastern Washington University, Cheney, Washington 99004, USA

⁹Department of Chemistry, North Carolina State University, Raleigh, North Carolina 27695-8204, USA

(Received 2 June 2016; revised manuscript received 18 November 2016; published 28 March 2017)

We combined magneto-infrared spectroscopy and first-principles calculations to unravel the role of spin-phonon coupling in the vicinity of the magnetic field-driven phase transitions in two chemically similar $S = 1/2$ Heisenberg antiferromagnets, $\text{CuF}_2(\text{H}_2\text{O})_2(3\text{-Clpy})$ and $[\text{Cu}(\text{pyz})_2(\text{HF}_2)]\text{PF}_6$. This comparison resolves questions about the conditions under which the lattice participates in magnetic-field-driven transitions and, at the same time, provides a way to predict how the lattice is likely to support microscopic spin rearrangements.

DOI: 10.1103/PhysRevB.95.104437

I. INTRODUCTION

Copper halide coordination polymers provide a superb platform for fundamental investigations of quantum phase transitions due to their overall low energy scales and simple tunable chemical structures [1–9]. The field-driven antiferromagnetic \rightarrow fully polarized state transition is a classic example [10,11]. While high field magnetization and microscopic modeling demonstrate that magnetic interactions dominate this process [11–13], magnetically driven transitions are not always spin-only processes. There is, for instance, plenty of evidence suggesting that spin and lattice can be inextricably linked [14–19]—at least under certain circumstances—although a test to determine the requirements for a lattice contribution has, so far, been missing. Two $S = 1/2$ Heisenberg antiferromagnets, $[\text{Cu}(\text{pyz})_2(\text{HF}_2)]\text{PF}_6$ and $\text{CuF}_2(\text{H}_2\text{O})_2(3\text{-Clpy})$, provide an opportunity to unravel this puzzle (Fig. 1). They display many chemical similarities including copper centers and soft flexible ligands (halides like F and Cl; rings like pyrazine and pyridine) that act as superexchange ligands and engage in hydrogen bonding. While both sport magnetic saturation transitions (at 37 and 24 T) [20,21], their different physical structures (Fig. 1) make it possible to unveil the role of specific local lattice distortions. To our surprise, this analysis affords a way to predict, in advance of any measurement, how the lattice supports microscopic spin rearrangements.

In this article, we explore spin-lattice coupling in $[\text{Cu}(\text{pyz})_2(\text{HF}_2)]\text{PF}_6$ and $\text{CuF}_2(\text{H}_2\text{O})_2(3\text{-Clpy})$ in order to test and for the first time delineate the conditions under which local lattice distortions are required to stabilize the fully polarized magnetic state. We find that while out-of-plane pyrazine ring distortions reinforce the magnetic saturation transition in quasi-two-dimensional $[\text{Cu}(\text{pyz})_2(\text{HF}_2)]\text{PF}_6$, spin-lattice coupling is strikingly absent in $\text{CuF}_2(\text{H}_2\text{O})_2(3\text{-Clpy})$. The difference arises from the fact that $[\text{Cu}(\text{pyz})_2(\text{HF}_2)]\text{PF}_6$ has ligands linking the magnetic centers that distort in order to

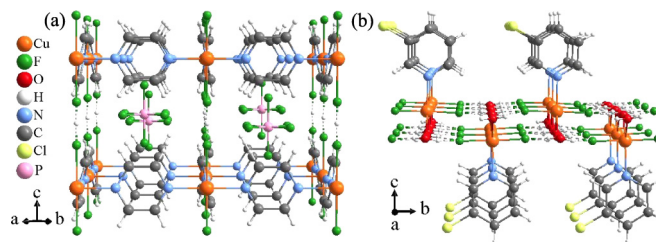


FIG. 1. (a) Crystal structure of quasi-two-dimensional $[\text{Cu}(\text{pyz})_2(\text{HF}_2)]\text{PF}_6$ [22]. This tetragonal system has robust atom- \cdots -atom linkages in the plane. These Cu-pyrazine layers are held together in the interlayer direction by hydrogen-bonded HF_2 ligands while the PF_6^- counterion sits in the cation pocket. The primary magnetic superexchange takes place via in-plane Cu-pyrazine-Cu linkages. (b) Crystal structure of $\text{CuF}_2(\text{H}_2\text{O})_2(3\text{-Clpy})$ [21]. This monoclinic system is molecular in nature, held together by hydrogen bonding and van der Waals interactions. The most important magnetic exchange pathway involves $\text{OH} \cdots \text{F}$ hydrogen bonds.

reduce the overall energy of the high field state, whereas $\text{CuF}_2(\text{H}_2\text{O})_2(3\text{-Clpy})$ is molecular, and, as a result, intermolecular hydrogen bonding alone provides for magnetic exchange and supports the fully polarized state. In addition to unveiling the circumstances under which energy transfer between the spin and lattice is relevant, these ideas can be used to anticipate the cooperative role of the lattice in other quantum materials. As examples, we discuss the magnetization steps in $\text{SrCu}_2(\text{BO}_3)_2$ and CdCr_2O_4 [23,24], the blocking temperature in Mn_{12} -acetate [25,26], and the sublattice coalescence in bimetallic $[\text{Ru}_2(\text{O}_2\text{CCH}_3)_4]_3[\text{Cr}(\text{CN})_6]$ [27] among others.

Single crystals were prepared by aqueous reaction as reported in Refs. [21,28] and suspended in polyethylene or KBr in polycrystalline form to control the optical density. Infrared transmission ($30\text{--}5000\text{ cm}^{-1}$) was carried out as a function

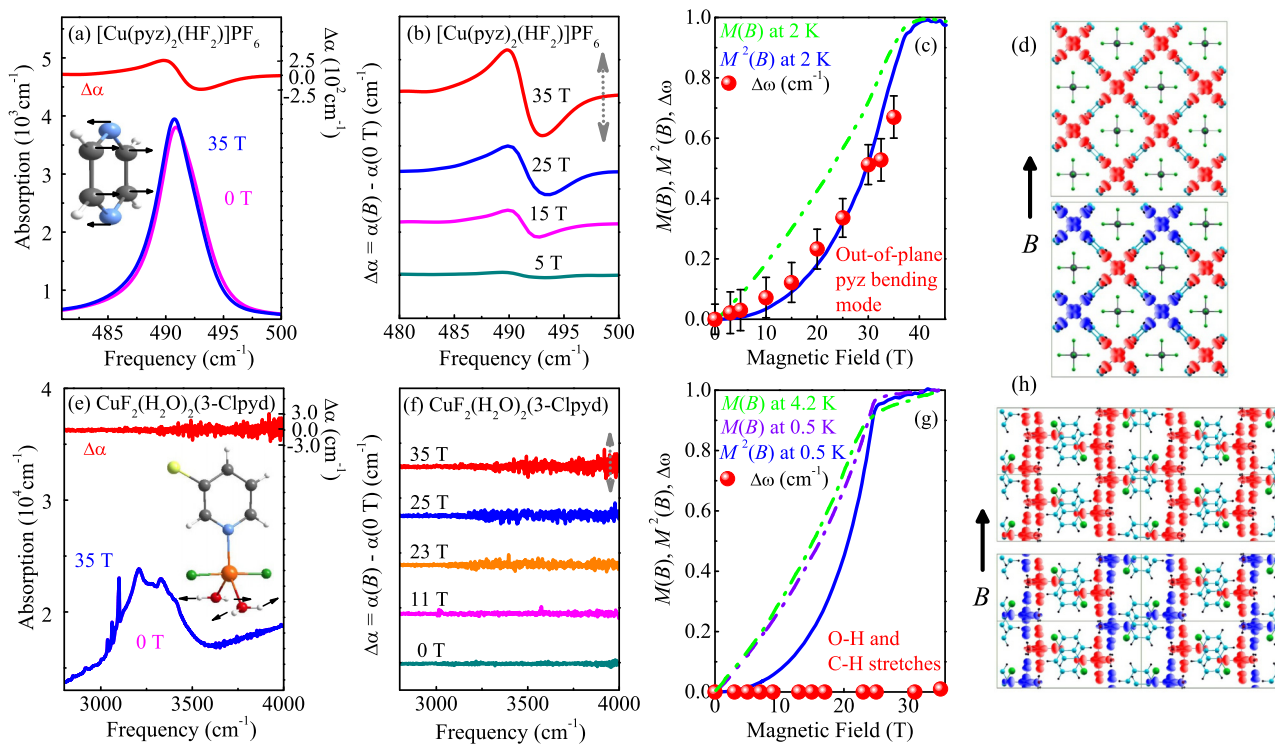


FIG. 2. (a) Close-up view of the absorption of $[\text{Cu}(\text{pyz})_2(\text{HF}_2)]\text{PF}_6$ at 0 and 35 T along with the full field absorption difference spectrum at 4.2 K. The latter is defined as $\Delta\alpha = \alpha(\omega, B) - \alpha(\omega, B = 0\text{T})$. (b) Waterfall plot of the absorption difference spectra with increasing field. A dashed gray 500- cm^{-1} scale bar is indicated. (c) The field-induced frequency shift of the 491- cm^{-1} out-of-plane pyrazine bending mode as a function of applied field along with magnetization [20] and the square of the magnetization. (d) Calculated spin-density distributions in the antiferromagnetic and ferromagnetic states of $[\text{Cu}(\text{pyz})_2(\text{HF}_2)]\text{PF}_6$. (e) Close-up view of the absorption of $\text{CuF}_2(\text{H}_2\text{O})_2(3\text{-Clpy})$ in the vicinity of the O-H and C-H stretch modes at 0 and 35 T along with the full field absorption difference spectrum at 4.2 K. (f) Absorption difference of this system with increasing magnetic field. Here, the dashed gray scale bar is 10 cm^{-1} . (g) The field-induced frequency shift of $\text{CuF}_2(\text{H}_2\text{O})_2(3\text{-Clpy})$ in the vicinity of the O-H and C-H stretching modes as a function of applied field compared with magnetization [21] and magnetization squared. (h) Calculated spin-density distributions in the antiferromagnetic and ferromagnetic states of $\text{CuF}_2(\text{H}_2\text{O})_2(3\text{-Clpy})$.

of temperature, and absorption was calculated as $\alpha(\omega) = -\frac{1}{cd} \ln[T(\omega)]$, where $T(\omega)$ is the measured transmittance, c is the concentration, and d is the thickness. The multiplex advantage in Fourier transform infrared spectroscopy allows simultaneous collection of data across a wide spectral range. We therefore had no need to focus on one mode or another during an experiment because—by default—the response of all infrared active modes is obtained at the same time. We performed magneto-infrared experiments at the National High Magnetic Field Laboratory (4.2 K, 0–35 T). Absorption differences, $\Delta\alpha = \alpha(\omega, B) - \alpha(\omega, B = 0\text{T})$, were calculated in order to highlight field-induced effects. Standard peak fitting techniques were employed as appropriate. Spin-density distributions for the antiferromagnetic and ferromagnetic states were calculated using density-functional theory and the Vienna *ab initio* simulation package [18,29–33].

II. RESULTS AND DISCUSSION

Figure 2 summarizes the magneto-infrared response of $[\text{Cu}(\text{pyz})_2(\text{HF}_2)]\text{PF}_6$ and $\text{CuF}_2(\text{H}_2\text{O})_2(3\text{-Clpy})$ in the vicinity of the 37 and 24 T magnetic phase transitions. Traditionally, local lattice distortions accompany this type of field-driven transition in copper halide coordination polymers. This occurs

to lower J_{AFM} and stabilize the fully polarized state [18,19]. We therefore focus on the vibrational modes that are related to important superexchange pathways in these materials.

Figure 2(a) displays a close-up view of the absolute absorption and full field absorption difference for the out-of-plane pyrazine bending mode near 490 cm^{-1} in $[\text{Cu}(\text{pyz})_2(\text{HF}_2)]\text{PF}_6$. This feature softens with applied field—consistent with expectations for a frequency shift. Moreover, the derivative-like structure in the absorption difference spectrum develops gradually and grows systematically with increasing field [Fig. 2(b)]. The changes are on the order of 12% at 35 T. All other modes are rigid (with the exception of the higher frequency out-of-plane pyrazine bend). In order to quantify these effects, we determined the field-induced shift of the 490- cm^{-1} mode as a function of field. These results are summarized in Fig. 2(c) where they are compared with the previously reported magnetization [20].

The standard scaling model [34] relates the square of the magnetization to the frequency shift as $M^2(B) \sim \Delta\omega \sim \omega(B) - \omega(B = 0\text{T})$. As shown in Fig. 2(c), the spectral data are in excellent agreement with the predicted trend. This indicates that field-induced changes in the out-of-plane pyrazine bending mode connect the lattice to the primary effect, which is spin canting and (eventually) development of

the fully polarized state. At the same time, the corresponding spin densities of $[\text{Cu}(\text{pyz})_2(\text{HF}_2)]\text{PF}_6$ are predicted to be out of phase and in phase for the antiferromagnetic and ferromagnetic states, respectively [Fig. 2(d)]. The spin density resides on the metal centers and pyrazine linkers in both states, so it makes sense that applied field primarily affects modes that modulate the exchange integral. The field-induced frequency shift also provides a chance to estimate the spin-phonon coupling constant as $\omega = \omega_0 + \lambda \langle S_i \cdot S_j \rangle$ [35,36]. Here ω and ω_0 are the perturbed and unperturbed frequencies, λ is the coupling constant, and $\langle S_i \cdot S_j \rangle$ is the spin-spin correlation function. Assuming a limiting low temperature value of S^2 for $\langle S_i \cdot S_j \rangle$ and a frequency shift of 0.5 cm^{-1} , we find that λ is on the order of 2 cm^{-1} . Finally, we point out that based on the relationship between $\Delta\omega$ and $M^2(B)$, the spin-lattice interactions are anticipated to saturate above 37 T where the antiferromagnetic \rightarrow fully polarized state transition is complete [20]. This is just beyond the current range of available powered magnets (35 T).

Comparison with $\text{CuF}_2(\text{H}_2\text{O})_2(3\text{-Clpy})$ provides an opportunity to test whether local lattice distortions support the magnetically driven phase transition in a purely molecular system [37]. Strikingly, none of the infrared-active vibrational modes change across the 24 T transition. This includes the F-Cu-F symmetric stretch, the O-Cu-O asymmetric bend, the out-of-plane pyridine bend, and the libration of the 3-chloropyridine ring around the C-Cl bond—all of which are important in the pressure-induced magnetic crossover [38]. Figure 2(e) shows a close-up view of the superimposed O-H and C-H stretches. Even at full field, the frequency shift $\Delta\omega = \omega(B = 35 \text{ T}) - \omega(B = 0 \text{ T})$ is zero within our sensitivity, which is better than 1%. This demonstrates that the O-H stretching mode (which is a superb local probe of the OH \cdots F superexchange pathway) does not participate in the field-driven antiferromagnetic \rightarrow fully polarized state transition at 24 T. In other words, the field-driven out-of-phase \rightarrow in-phase spin density on the two-dimensional hydrogen bonded sheets is not coupled to the aforementioned vibrational modes, even though our spin-density calculations predict the characteristic patterns [Fig. 2(h)]. We therefore surmise that the local lattice distortions that are required to lower J_{AFM} in $[\text{Cu}(\text{pyz})_2(\text{HF}_2)]\text{PF}_6$ and many other molecule-based materials [18,19] are not needed here. This is because magnetic exchange in $\text{CuF}_2(\text{H}_2\text{O})_2(3\text{-Clpy})$ is wholly determined by the hydrogen bonding network [21]. This finding is consistent with the mechanism of the antiferromagnetic \rightarrow ferromagnetic crossover under compression which is driven by dimensional-switching of the hydrogen bonding network [38].

One of the outcomes of this work with copper halide coordination polymers is the ability to more broadly anticipate the role of the lattice in the magnetic transitions of other quantum materials. This capability is based on the finding that superexchange through chemical bonds requires a distortion, whereas that through space does not. It clearly does not apply to every circumstance, but there are many instances where this insight will be useful. For example, $\text{SrCu}_2(\text{BO}_3)_2$ and CdCr_2O_4 are extended solids with important metal-oxygen-metal exchange pathways that are well known for their magnetic-field-induced transitions and, in particular, the various plateau states that are manifest as steps in the magnetization [23,24].

The lattice connectivity between metal centers immediately portends cooperative spin-lattice effects, which is exactly what is observed [24,39,40]. In other words, because the exchange interaction J goes as t^2/U , where t is the transfer integral ($\int \phi_i H \phi_j d\tau$) and U is the on-site Coulomb interactions, it is natural that field-induced changes in the microscopic spin state impact bond length and angles and vice versa [41]. Another system of contemporary interest is the multiferroic metal-organic framework $[(\text{CH}_3)_2\text{NH}_2]\text{Mn}(\text{HCOO})_3$ [42]. Based on its metal \cdots ligand \cdots metal connectivity, we anticipate spin-lattice interactions involving the formate group. This remains to be tested.

The molecular magnet Mn_{12} -acetate is different. It sports quantum tunneling and a 3 K blocking temperature [25,26]. While there is modest spin-lattice coupling due to modulation of the exchange integral by a few intramolecular vibrations [43], there are no field-induced changes in the intermolecular interactions of this system, and we predict that the lattice is rigid across the blocking temperature. As a second example, we consider the unusual interpenetrating lattice structure in bimetallic $[\text{Ru}_2(\text{O}_2\text{CCH}_3)_4]_3[\text{Cr}(\text{CN})_6]$ [27]. There is practically no coupling between the two spin sublattices so there are many degenerate configurations, which can be aligned by an 0.08 T magnetic field [44]. This compound thus represents an interesting example of a three-dimensional system with frustration that can be lifted by external stimuli. Based on connectivity issues, it is not surprising that there is no evidence for spin-lattice coupling in $[\text{Ru}_2(\text{O}_2\text{CCH}_3)_4]_3[\text{Cr}(\text{CN})_6]$ across the 0.7 T magnetic sublattice coalescence because it involves independent magnetic frameworks [45]. Finally, we point out emerging interest in the molecule-based multiferroic $(\text{NH}_4)_2\text{FeCl}_5 \cdot \text{H}_2\text{O}$ [46]. Based on an analysis of this system, we predict modest spin-phonon coupling.

We now turn briefly to temperature effects. Figure 3 brings together the variable-temperature infrared response of $[\text{Cu}(\text{pyz})_2(\text{HF}_2)]\text{PF}_6$. Analysis of peak shifts and splittings reveals the presence of a weak structural distortion around 75 K. The most important point is that these changes primarily involve the pyrazine ligand. The cluster near 850 cm^{-1} (which represents the out-of-plane C-H bending mode of the pyrazine ring) is a perfect example of this effect. It has one component that softens through T_c , another branch that is relatively insensitive, and a third that splits into a clear triplet below 75 K, indicating a structural component to this transition. The Cu center is also affected to the extent that it is modulated by the surrounding ligands. These subtle modifications act to stabilize the low-temperature long-range ordered state although there is no spin-lattice coupling across T_N within our sensitivity. Getting back to the overall temperature trend, we point out that modulation of the exchange integral by lattice vibrations may lead to temperature dependence of exchange constants [14]. By contrast, $\text{CuF}_2(\text{H}_2\text{O})_2(3\text{-Clpy})$ shows no evidence of structural changes or local lattice distortions down to 4.2 K [38]. This is further support that local lattice distortions are necessary when atom-atom linkages are present but of lesser importance when superexchange occurs via intermolecular interactions.

To summarize, we have drawn together the vibrational and magnetic response of two chemically similar $S = 1/2$ Heisenberg antiferromagnets to determine the conditions under which local lattice distortions participate in a magnetic

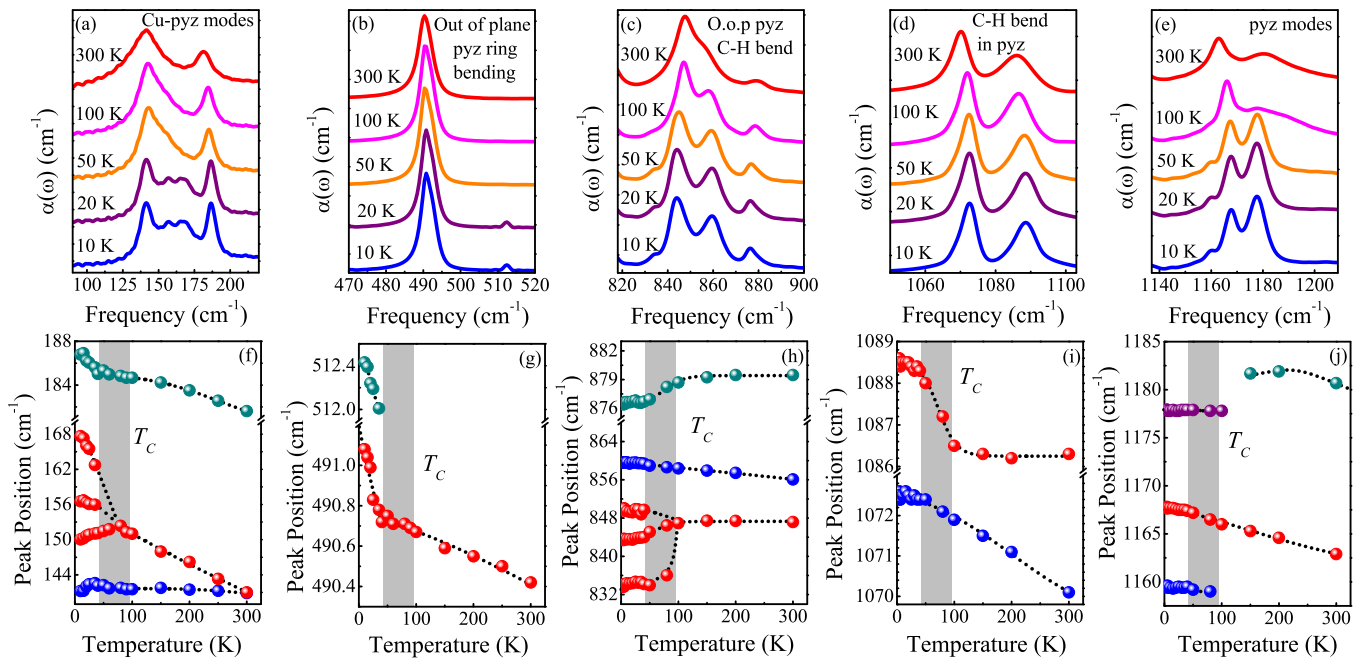


FIG. 3. [(a)–(e)] Close-up view of selected infrared-active vibrational modes of $[\text{Cu}(\text{pyz})_2(\text{HF}_2)]\text{PF}_6$ as a function of temperature along with their mode assignments. The curves are offset for clarity. [(f)–(j)] Frequency vs. temperature for the same features. Vibrational changes near 75 K are due to local lattice distortions. The gray band near 75 K denotes the transition region.

phase transition. We find that while the pyrazine ligands distort to reduce the antiferromagnetic exchange and stabilize the fully polarized state in $[\text{Cu}(\text{pyz})_2(\text{HF}_2)]\text{PF}_6$, the OH stretch in $\text{CuF}_2(\text{H}_2\text{O})_2(3\text{-Clpy})$ (and all other ligands involved in intermolecular hydrogen bonding) are rigid. This comparison shows, in a very dramatic manner, that striction is not an essential aspect of the magnetic phase transition in these materials unless there are robust atom-atom linkages involved in the superexchange pathway. We illustrate the breadth and utility of these simple ideas with predictions for several other quantum materials: $\text{SrCu}_2(\text{BO}_3)_2$ and CdCr_2O_4 (where magnetization steps take place with changes in the lattice) [24,39,40] and the blocking temperature in Mn_{12} -acetate and

sublattice coalescence in $[\text{Ru}_2(\text{O}_2\text{CCH}_3)_4]_3[\text{Cr}(\text{CN})_6]$ [45] which are uncorrelated with the structure.

ACKNOWLEDGMENTS

Research at the University of Tennessee and Eastern Washington University is supported by the National Science Foundation (Grants No. DMR-1063880 and No. DMR-1306158, respectively). A portion of this research was performed at the National High Magnetic Field Laboratory, which is supported by the National Science Foundation Cooperative Agreement DMR-1157490, the State of Florida, and the U.S. Department of Energy.

- [1] P. Coleman and A. J. Schofield, *Nature* **433**, 226 (2005).
- [2] P. A. Goddard, J. L. Manson, J. Singleton, I. Franke, T. Lancaster, A. J. Steele, S. J. Blundell, C. Baines, F. L. Pratt, R. D. McDonald, O. E. Ayala-Valenzuela, J. F. Corbey, H. I. Southerland, P. Sengupta, and J. A. Schlueter, *Phys. Rev. Lett.* **108**, 077208 (2012).
- [3] M. B. Stone, D. H. Reich, C. Broholm, K. Lefmann, C. Rischel, C. P. Landee, and M. M. Turnbull, *Phys. Rev. Lett.* **91**, 037205 (2003).
- [4] S. Sachdev, *Nat. Phys.* **4**, 173 (2008).
- [5] M. Ozerov, A. A. Zvyagin, E. Čížmár, J. Wosniza, R. Feyerherm, F. Xiao, C. P. Landee, and S. A. Zvyagin, *Phys. Rev. B* **82**, 014416 (2010).
- [6] C. P. Landee and M. M. Turnbull, *Eur. J. Inorg. Chem.* **2013**, 2266 (2013).
- [7] C. P. Landee and M. M. Turnbull, *J. Coord. Chem.* **67**, 375 (2014).
- [8] M. Conner, A. McConnell, J. Schlueter, and J. Manson, *J. Low Temp. Phys.* **142**, 277 (2006).
- [9] S. Sachdev and B. Keimer, *Phys. Today* **64**, 29 (2011).
- [10] Y. Kono, T. Sakakibara, C. P. Aoyama, C. Hotta, M. M. Turnbull, C. P. Landee, and Y. Takano, *Phys. Rev. Lett.* **114**, 037202 (2015).
- [11] P. A. Goddard, J. Singleton, P. Sengupta, R. D. McDonald, T. Lancaster, S. J. Blundell, F. L. Pratt, S. Cox, N. Harrison, J. L. Manson, H. I. Southerland, and J. A. Schlueter, *New J. Phys.* **10**, 083025 (2008).
- [12] C. Yasuda, S. Todo, K. Hukushima, F. Alet, M. Keller, M. Troyer, and H. Takayama, *Phys. Rev. Lett.* **94**, 217201 (2005).

- [13] K. Balamurugan, S.-H. Lee, J.-S. Kim, J.-M. Ok, Y.-J. Jo, Y.-M. Song, S.-A. Kim, E. S. Choi, M. D. Le, and J.-G. Park, *Phys. Rev. B* **90**, 104412 (2014).
- [14] M. Klanjšek, D. Arčon, A. Sans, P. Adler, M. Jansen, and C. Felser, *Phys. Rev. Lett.* **115**, 057205 (2015).
- [15] J. Rohrkamp, M. D. Phillips, M. M. Turnbull, and T. Lorenz, *J. Phys. Conf. Ser.* **200**, 012169 (2010).
- [16] P. R. Hammar, M. B. Stone, D. H. Reich, C. Broholm, P. J. Gibson, M. M. Turnbull, C. P. Landee, and M. Oshikawa, *Phys. Rev. B* **59**, 1008 (1999).
- [17] A. V. Sologubenko, K. Berggold, T. Lorenz, A. Rosch, E. Shimshoni, M. D. Phillips, and M. M. Turnbull, *Phys. Rev. Lett.* **98**, 107201 (2007).
- [18] J. L. Musfeldt, L. I. Vergara, T. V. Brinzari, C. Lee, L. C. Tung, J. Kang, Y. J. Wang, J. A. Schlueter, J. L. Manson, and M.-H. Whangbo, *Phys. Rev. Lett.* **103**, 157401 (2009).
- [19] Ö. Günaydin-Şen, C. Lee, L. C. Tung, P. Chen, M. M. Turnbull, C. P. Landee, Y. J. Wang, M. H. Whangbo, and J. L. Musfeldt, *Phys. Rev. B* **81**, 104307 (2010).
- [20] E. Čížmár, S. A. Zvyagin, R. Beyer, M. Uhlarz, M. Ozerov, Y. Skourski, J. L. Manson, J. A. Schlueter, and J. Wosnitza, *Phys. Rev. B* **81**, 064422 (2010).
- [21] S. H. Lapidus, J. L. Manson, H. Park, A. J. Clement, S. Ghannadzadeh, P. Goddard, T. Lancaster, J. S. Möller, S. J. Blundell, M. T. F. Telling, J. Kang, M.-H. Whangbo, and J. A. Schlueter, *Chem. Commun.* **49**, 499 (2013).
- [22] J. L. Manson, J. A. Schlueter, K. A. Funk, H. I. Southerland, B. Twamley, T. Lancaster, S. J. Blundell, P. J. Baker, F. L. Pratt, J. Singleton, R. D. McDonald, P. A. Goddard, P. Sengupta, C. D. Batista, L. Ding, M. Whangbo, I. Franke, S. Cox, C. Baines, and D. Trial, *J. Am. Chem. Soc.* **131**, 6733 (2009).
- [23] M. Jaime, R. Daou, S. A. Crooker, F. Weickert, A. Uchida, A. E. Feiguin, C. D. Batista, H. A. Dabkowska, and B. D. Gaulin, *Proc. Natl. Acad. Sci. USA* **109**, 12404 (2012).
- [24] H. Ueda, H. A. Katori, H. Mitamura, T. Goto, and H. Takagi, *Phys. Rev. Lett.* **94**, 047202 (2005).
- [25] R. Sessoli, D. Gatteschi, A. Caneschi, and M. A. Novak, *Nature* **365**, 141 (1993).
- [26] J. M. Hernandez, X. X. Zhang, F. Luis, J. Tejada, J. R. Friedman, M. P. Sarachik, and R. Ziolo, *Phys. Rev. B* **55**, 5858 (1997).
- [27] J. S. Miller, T. E. Vos, and W. W. Shum, *Adv. Mater.* **17**, 2251 (2005).
- [28] J. L. Manson, M. M. Conner, J. A. Schlueter, T. Lancaster, S. J. Blundell, M. L. Brooks, F. L. Pratt, T. Papageorgiou, A. D. Bianchi, J. Wosnitza, and M.-H. Whangbo, *Chem. Commun.* **47**, 4894 (2006).
- [29] P. E. Blöchl, *Phys. Rev. B* **50**, 17953 (1994).
- [30] S. L. Dudarev, G. A. Botton, S. Y. Savrasov, C. J. Humphreys, and A. P. Sutton, *Phys. Rev. B* **57**, 1505 (1998).
- [31] G. Kresse and D. Joubert, *Phys. Rev. B* **59**, 1758 (1999).
- [32] G. Kresse and J. Furthmüller, *Phys. Rev. B* **54**, 11169 (1996).
- [33] J. P. Perdew, K. Burke, and M. Ernzerhof, *Phys. Rev. Lett.* **77**, 3865 (1996).
- [34] E. Granado, A. García, J. A. Sanjurjo, C. Rettori, I. Torriani, F. Prado, R. D. Sánchez, A. Caneiro, and S. B. Oseroff, *Phys. Rev. B* **60**, 11879 (1999).
- [35] C. J. Fennie and K. M. Rabe, *Phys. Rev. Lett.* **96**, 205505 (2006).
- [36] A. B. Sushkov, O. Tchernyshyov, W. Ratcliff, S. W. Cheong, and H. D. Drew, *Phys. Rev. Lett.* **94**, 137202 (2005).
- [37] The magneto-infrared response of $\text{CuF}_2(\text{H}_2\text{O})_2(3\text{-Clpy})$ was measured above the 2.1 K Néel temperature. It is, however, well established that spin-spin correlations in copper halides are quite robust—even above the ordering temperature [11,21]. Inspection of the magnetization above the ordering temperature shows a strong remnant of the antiferromagnetic \rightarrow fully polarized state transition—with no evidence for spin-lattice coupling.
- [38] K. R. O’Neal, T. V. Brinzari, J. B. Wright, C. Ma, S. Giri, J. a Schlueter, Q. Wang, P. Jena, Z. Liu, and J. L. Musfeldt, *Sci. Rep.* **4**, 6054 (2014).
- [39] Y. Narumi, N. Terada, Y. Tanaka, M. Iwaki, K. Katsumata, K. Kindo, H. Kageyama, Y. Ueda, H. Toyokawa, T. Ishikawa, and H. Kitamura, *J. Phys. Soc. Jpn.* **78**, 043702 (2009).
- [40] G. Radtke, A. Saúl, J. A. Dabkowska, M. B. Salamon, and M. Jaime, *Proc. Nat. Acad. Sci. USA* **112**, 1971 (2015).
- [41] J. B. Goodenough, *Magnetism and the Chemical Bond* (Interscience and John Wiley, New York, 1963).
- [42] P. Jain, V. Ramachandran, R. J. Clark, D. Z. Hai, B. H. Toby, N. S. Dalal, H. W. Kroto, and A. K. Cheetham, *J. Am. Chem. Soc.* **131**, 13625 (2009).
- [43] A. B. Sushkov, B. R. Jones, J. L. Musfeldt, Y. J. Wang, R. M. Achey, and N. S. Dalal, *Phys. Rev. B* **63**, 214408 (2001).
- [44] R. S. Fishman, W. W. Shum, and J. S. Miller, *Phys. Rev. B* **81**, 172407 (2010).
- [45] T. V. Brinzari, P. Chen, L.-C. Tung, Y. Kim, D. Smirnov, J. Singleton, J. S. Miller, and J. L. Musfeldt, *Phys. Rev. B* **86**, 214411 (2012).
- [46] M. Ackermann, D. Brüning, T. Lorenz, P. Becker, and L. Bohatý, *New J. Phys.* **15**, 123001 (2013).